Science of the Total Environment 715 (2020) 136927

Contents lists available at ScienceDirect

Science of the Total Environment

journal homepage: www.elsevier.com/locate/scitotenv

# Analysis of engineered nanomaterials (Ag, $CeO_2$ and $Fe_2O_3$) in spiked surface waters at environmentally relevant particle concentrations

Frédéric Loosli *, Jingjing Wang, Mithun Sikder, Kamelia Afshinnia, Mohammed Baalousha *

*Center for Environmental Nanoscience and Risk, Department of Environmental Health Sciences, Arnold School of Public Health, University of South Carolina, Columbia, SC, United States*

## HIGHLIGHTS

- Efficient extraction of nanomaterials from synthetic and natural waters
- Quantification of metal and metal oxide ENMs in natural surface waters
- Element ratios permit to quantify engineered nanomaterials (ENMs) in surface waters.
- Multi-method approach is required to fill gap in ENM characterization in natural samples

## GRAPHICAL ABSTRACT

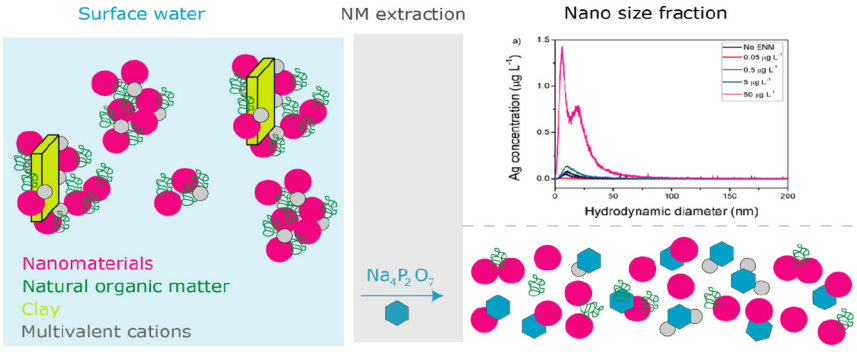


## ARTICLE INFO

*Article history:*
Received 13 December 2019
Received in revised form 23 January 2020
Accepted 23 January 2020
Available online 25 January 2020

Editor: Damia Barcelo

*Keywords:*
Nanomaterial extraction
Nanomaterial characterization
Engineered nanomaterial quantification
AF4-ICP-MS
sp-ICP-MS, sodium pyrophosphate

## ABSTRACT

Quantification of engineered nanomaterials (ENMs) concentrations in surface waters remains one of the key challenges in environmental nanoscience and nanotechnology. A promising approach to estimate metal and metal oxide ENM concentrations in complex environmental samples is based on the increase in the elemental ratios of ENM-contaminated samples relative to the corresponding natural background elemental ratios. This contribution evaluated the detection and quantification of Ag, $CeO_2$, and $Fe_2O_3$ ENMs spiked in synthetic soft, or in natural river waters using the elemental ratio approach, and evaluated the effect of extractants including sodium hydroxide (NaOH), sodium oxalate ($Na_2C_2O_4$) and sodium pyrophosphate ($Na_4P_2O_7$) on the recovery of ENMs from the spiked waters. The extracted ENM concentrations were higher in $Na_4P_2O_7$-extracted suspensions than in NaOH- and $Na_2C_2O_4$-extracted suspensions due to the higher efficiency of $Na_4P_2O_7$ to break up natural and engineered nanomaterial heteroaggregates. The size distributions of the extracted suspensions were determined by asymmetrical flow-field flow fractionation coupled to inductively coupled plasma-mass spectrometer (AF4-ICP-MS). These size distribution analysis demonstrated that Ag ENMs were extracted from the spiked river water as both primary particles and small (<100 nm) aggregates, whereas $CeO_2$ ENMs were extracted from the spiked river water as aggregates of particles in the size range 0–200 nm. The number particle size distribution of the extracted suspensions confirmed that Ag ENMs were extracted as a mixture of primary and aggregated Ag ENMs. Small Ag ENMs (*i.e.* <20 nm) were detected by AF4-ICP-MS, but these particles were not detected by single particle (sp)-ICP-MS due to high size detection limit of sp-ICP-MS. This study illustrates that the elemental ratio approach is a promising approach to detect and quantify ENMs in surface waters. This study also illustrates the need for a multi-method approach, including extraction, filtration, AF4-ICP-MS and sp-ICP-MS, to detect, quantify, and characterize ENMs in surface waters.



* Corresponding authors.
*E-mail addresses:* looslifred@gmail.com (F. Loosli), mbaalous@mailbox.sc.edu (M. Baalousha).

https://doi.org/10.1016/j.scitotenv.2020.136927
0048-9697/

## 1. Introduction

Measuring the concentrations of engineered nanomaterials (ENMs) in surface waters is essential to evaluate the potential risks, and to calibrate and validate ENM fate models (Lead et al., 2018). However, the current knowledge on environmental concentrations of ENMs is largely based on ENM fate models which have not been parameterized and/or validated against field measurements (Baalousha et al., 2016; Nowack et al., 2015). Currently, few studies reported measured ENM concentrations in environmental systems (*e.g.*, surface waters and soils) (Gondikas et al., 2014; Loosli et al., 2019a; Reed et al., 2017). For instance, the average concentration of $TiO_2$ ENMs in the Old Danube lake (Vienna, Austria) water during a year period increased from 1.7 μg $L^{-1}$ in winter to 27.1 μg $L^{-1}$ in summer due to $TiO_2$ input from sunscreens (Gondikas et al., 2014). Low concentrations of $TiO_2$ ENMs, in the range of 0.4–110 ng $L^{-1}$, were measured in Clear Creek in Golden, Colorado during summer due to $TiO_2$ input from sunscreens (Reed et al., 2017). The sparse data on measured ENM environmental concentrations can be attributed to the complexity of ENM analysis in complex environmental samples. Measuring the concentrations of ENMs in surface waters can be impeded by the low expected ENM concentrations (*e.g.*, ng $L^{-1}$ to μg $L^{-1}$ range) in surface waters (Gondikas et al., 2018; Reed et al., 2017); the high background concentration of natural nanomaterials (NNMs, high μg $L^{-1}$ to mg $L^{-1}$ range), often with the similar elemental composition as ENMs (*e.g.*, $CeO_2$, and $TiO_2$); the similarity of the physicochemical properties (*e.g.*, size and composition) of ENMs and NNMs; the heteroaggregation of ENMs and NNMs; and the underdeveloped methodologies to accurately characterize ENMs and NNMs with sufficient specificity and sensitivity (von der Kammer et al., 2012).

Among the most promising analytical techniques for the detection and quantification of metal and metal oxide ENMs at environmentally relevant concentrations (*e.g.*, ng $L^{-1}$ to μg $L^{-1}$) are conventional- and single particle- inductively coupled plasma-mass spectrometer (sp-ICP-MS) and asymmetrical flow-field flow fractionation (AF4) coupled to ICP-MS. These techniques have shown great potential in detecting ENMs (*e.g.*, Ag ENMs, $TiO_2$, and Fe oxides ENMs) in the aquatic and terrestrial environments (Gondikas et al., 2014; Praetorius et al., 2017; von der Kammer et al., 2012). When coupled with ICP-MS, AF4 measures element-based particle size distribution, from which elemental ratios (*e.g.* Ce/La, Ti/Nb, etc.) can be calculated as a function of particle size (Baalousha et al., 2006). Thus, AF4-ICP-MS could enable differentiating ENMs from NNMs based on their size-dependent elemental ratios. Additionally, sp-ICP-MS analysis of environmental samples can be of interest to measure particle number concentration and number size distribution on individual particle basis, and has been implemented for detection of ENMs in environmental media (Gondikas et al., 2018; Navratilova et al., 2015; Praetorius et al., 2017; Venkatesan et al., 2018).

Most studies investigating ENM detection and quantification separated ENMs from the environmental matrices by simple filtration and/or centrifugation in order to reduce particle polydispersity prior analysis *e.g.*, by sp-ICP-MS and/or AF4 (Mozhayeva and Engelhard, 2020. However, sample filtration could lead to underestimation of the total ENM concentrations in a given sample because of the heteroaggregation of ENMs with natural particles. Dispersion of ENMs from ENM-natural particle heteroaggregates into their primary particles or into smaller aggregates (*e.g.* <100 nm) is thus essential to improve ENM detectability and quantification (Loosli et al., 2018). Regelink et al. suggested pyrophosphate as a more effective extractant to disperse iron oxide NNMs from soil compared to other extractants (*e.g.*, NaOH and NaCl) (Regelink et al., 2013). Similarly, we demonstrated that sodium pyrophosphate is the most efficient extractants compared to sodium hydroxide or sodium oxalate to extract NNMs from soils (*e.g.*, clays, iron, manganese, cerium, and titanium oxides) (Loosli et al., 2018).

This study aims to i) evaluate efficiency of extractants (*e.g.*, sodium hydroxide, sodium oxalate, and tetrasodium pyrophosphate) to disperse and extract ENMs from surface water samples spiked with Ag, $CeO_2$, and $Fe_2O_3$ ENMs, and ii) evaluate different approaches for the detection and quantification of ENMs in surface waters including elemental ratios following total sample digestion, size resolved elemental ratios using AF4-ICP-MS, and sp-ICP-MS.

## 2. Materials and methods

### 2.1. Synthesis and characterization of Ag ENMs

Ag ENMs were synthesized following a previously reported method (Römer et al., 2011). Briefly, 400 mL of ultrapure water (UPW, PURELAB Option-Q, ELGA) was brought to boiling in a glass conical flask. A solution of 1.69 mL of 58.8 mM silver nitrate was added to the boiling water followed by 2.92 mL of 34 mM sodium citrate (ACS reagent, Sigma-Aldrich®, USA), while stirring. Lastly, 2 mL of 100 mM freshly-prepared sodium borohydride (Purum p.a., Sigma-Aldrich®, USA) was added drop-wise to the mixture. The mixture was stirred for 15 min while boiling, then cooled slowly to room temperature while stirring for 45 min. Afterwards, Ag ENM suspension was cleaned using a $N_2$ gas-pressurized stirred ultrafiltration cell (Amicon®, 3 kDa regenerated cellulose membrane, Millipore) to remove the excess reagents. During the cleaning process, Ag ENM suspension volume was reduced to 200 mL and then replenished by 200 mL of 0.26 mM sodium citrate solution. This process was repeated four times to remove excess reagents.

The concentration of the synthesized citrate coated Ag ENMs was measured by inductively coupled plasma-optical emission spectroscopy (ICP-OES, Varian 710-ES, USA). The total Ag concentration of the stock suspension was 23.7 mg $L^{-1}$. The z-average hydrodynamic diameter and the zeta potential of Ag ENMs in the stock suspension (*e.g.*, 0.26 mM sodium citrate at pH 7.0) were determined by dynamic light scattering (DLS) and laser Doppler electrophoresis, respectively using a Malvern Zetasizer NanoZS Instrument (Malvern, USA) and are reported as the mean ± standard deviation of five replicates.

### 2.2. Cerium and iron oxide ENMs

$CeO_2$ ENMs suspensions were prepared using manufactured nanopowder supplied by the European Commission's Joint Research Centre (NM-212) (Singh et al., 2014). $Fe_2O_3$ ENMs were prepared by suspending the manufactured nanopowder purchased from Sigma Aldrich in UPW. $CeO_2$ and $Fe_2O_3$ ENM stock suspensions were prepared at ENM concentration of 625 mg $L^{-1}$ and were dispersed by sonication using a bath sonicator for 1 h (Branson Model 2800, 40 kHz, USA).

### 2.3. Evaluation of different sample preparation for measuring total ENM concentration

A comparison of three different sample preparation procedure for measuring total ENM concentration was conducted including: 1) dilution in UPW, 2) acidification using 2% nitric acid ($HNO_3$, Trace metal grade, Fisher Chemicals, Canada), and 3) sample digestion using hydrofluoric acid (HF). Aliquots of Ag, $CeO_2$, and $Fe_2O_3$ ENM stock suspensions were diluted to 50 μg $L^{-1}$. ENMs suspensions were sonicated for 1 h and the elemental concentration of the ENMs were determined by ICP-OES. For the samples in UPW, ENM suspensions were introduced directly to the ICP-OES. For the acidification treatment, the ENM suspensions and the 2% $HNO_3$ were introduced to the ICP-OES simultaneously using a T-junction connector to avoid altering ENM stability and thus to minimize sample losses due to sedimentation prior to injection to ICP-OES. Total ENM digestion was performed according to the procedure described in Section 2.6. All measurements were performed in triplicates and all results are reported as mean and standard deviation of the triplicate measurements.

### 2.4. ENM extraction from synthetic soft water

A set of experiments was performed in synthetic soft water (48 mg $L^{-1}$ $NaHCO_3$, 30 mg $L^{-1}$ $CaSO_4.2H_2O$, 30 mg $L^{-1}$ $MgSO_4$, and 2 mg $L^{-1}$ KCl) (US EPA, 2002) containing 5 mg $L^{-1}$ Suwannee River humic acid (SRHA, International Humic Substances Society, USA) in order to evaluate the extraction efficiency of sodium pyrophosphate ($Na_4P_2O_7$, analytical grade, Alfa Aesar, Japan) and sodium oxalate ($Na_2C_2O_4$, analytical grade, Alfa Aesar, China) in a simple media (synthetic soft water) in the absence of interferences from natural particles containing analogous NNMs and/or metals forming the ENMs. The synthetic soft water solution was prepared following the U.S. Environmental Protection Agency protocol (US EPA, 2002). A 100 mg $L^{-1}$ SRHA stock solution was prepared by dissolving 2 mg of freeze dried SRHA in 20 mL UPW. The pH was adjusted to 7.0 through addition of 0.1 or 1 M NaOH. The SRHA stock solution was filtered through a 100 nm filter (polyvinylidene difluoride membrane, Millex® Syringe Filter Unit, Millipore, USA), prior SRHA and ENM spiking into the synthetic water, to remove any aggregated SRHA molecules that did not fully dissolve during the preparation of the SRHA stock solution. ENMs (*e.g.*, final concentration of 55 μg $L^{-1}$ Ag, Fe and Ce) were spiked in a synthetic soft water containing 5 mg $L^{-1}$ SRHA and the resulting suspensions were overhead shaken using a tube rotator (Fisher Scientific, China) at 40 rpm for 24 h. ENMs were extracted by missing 36 mL of the ENM-spiked synthetic water with 4 mL of the extracting solution (*e.g.,* 5 mM NaOH, 20 and 100 mM $Na_2C_2O_4$, or 100 mM $Na_4P_2O_7$), resulting in final ENM concentration of 50 μg $L^{-1}$ Ag, Fe and Ce and final extractant concentrations of: i) 0.5 mM NaOH, ii) 2 and 10 mM $Na_2C_2O_4$, or iii) 2 and 10 mM $Na_4P_2O_7$. All final suspensions were adjusted to pH 10 using NaOH where needed, to enhance electrostatic repulsions between particles, and thus increase particle dispersion. The suspensions were overhead shaken with a tube rotator (Fisher Scientific, China) overnight at 40 rpm, followed by 1 h sonication in a bath sonicator (Branson, Model 2800, 40 kHz, USA). The sonicated suspensions were filtered using 450 nm syringe filters (polyethersulfone membrane, VWR, USA) membranes to obtain the size fraction <450 nm. The <100 nm fraction was obtained by filtering half of the <450 nm filtrates (around 20 mL) using 100 nm syringe filters (polyvinylidene difluoride membrane, Millex® Syringe Filter Unit, Millipore, USA). The filtrates (*e.g.*, <450 nm and < 100 nm size fractions) were acidified with 2% $HNO_3$ and analyzed by ICP-OES. The dissolved fractions (*i.e.*, the size fraction <3 kDa) were obtained by centrifugal ultrafiltration using Amicon® Ultra-4 filtration cartridges at 3 kDa membrane (regenerated cellulose, Millipore, USA). Samples were centrifuged at 4000 *g* for 20 min using an Eppendorf 5810R Centrifuge. Then the dissolved fractions were acidified using 2% $HNO_3$ and analyzed by inductively coupled plasma-mass spectrometry (ICP-MS, PerkinElmer NexION350D, USA).

### 2.5. NNM and ENM extraction from spiked river water

Two extraction protocols were applied to extract ENMs spiked in river water. River water sample was collected on October 2017 from Congaree River formed by the confluence of the Broad and Saluda rivers at Columbia, South Carolina, USA. The pH and conductivity of the water measured *in situ* were 7.8 and 106 μS $cm^{-1}$ (YSI, Professional Plus Multiparameter Meter, Xylem, USA), respectively. Element concentration (Ag, Ce, Fe and La) of the Congaree River water sampled is reported in Table S1 in the Supporting Information. NMs were also extracted from the natural river water in the presence of 10 mM $Na_4P_2O_7$ without spiked ENMs.

Stock solutions of 23.7 mg $L^{-1}$ Ag ENMs, 625 mg $L^{-1}$ $CeO_2$ and $Fe_2O_3$ ENMs, and 100 mM $Na_4P_2O_7$ were prepared. Aliquots of ENM stock suspensions were mixed together and diluted in UPW in order to prepare ENM mixtures at 0.1, 1.0, and 10 mg $L^{-1}$ Ag, Ce, and Fe. Aliquots of ENM mixtures were spiked in the River water to obtain final ENM concentrations of 0, 0.055, 0.55, 55, and 55 μg $L^{-1}$ (as Ag, Ce, and Fe) in the River water. The mixture of ENMs and river water were stirred for 48 h. Then, NM were extracted from the ENM-spiked river water by adding either 1) 4 mL of 100 mM $Na_4P_2O_7$, or 2) aliquots of NaOH to 36 mL of the ENM-spiked water samples. NaOH was added to adjust the extraction suspension to pH 10. The resulting mixtures were stirred overnight at 30 rpm in a tube rotator. Samples were then sonicated for 1 h and filtered with 450 and 100 nm membranes. The dissolved fraction was obtained by centrifugal ultrafiltration of the ENM-spiked waters using Amicon® Ultra-4 filtration cartridges at 3 kDa membrane (Millipore, USA) at 4000 g for 20 min. Finally, the <450 and < 100 nm fractions were HF digested (see Section 2.6 below for details of HF digestion protocol) and analyzed, in addition to the dissolved fraction, by ICP-MS.

### 2.6. Sample digestion and elemental analysis

Trace metal concentrations of the extracted <0.45 and < 0.1 μm suspensions from the river water (see Section 2.5) were determined by ICP-MS after digestion. The extracted suspensions were digested in 15 mL Teflon vessels (Savillex, USA) on custom-made Teflon covered hotplates placed in a box equipped with double-HEPA filtered forced air in a metal-free HEPA filtered air clean lab. A 5 mL water aliquot was placed in the vessel and weighted (Mettler Toledo, Excellence Plus, Switzerland). Samples were dried down at 110 °C and treated with 1 mL of 30% $H_2O_2$ (Fisher Chemical, USA) for 2 h at 70 °C to remove organic matter. $H_2O_2$ was then evaporated and the samples were digested with 2 mL of HF: $HNO_3$ (3:1) mixture (ACS grade acids distilled in the laboratory) for 24 h at 110 °C. After evaporation of the acid mixture at 110 °C, the residue was reacted with 1 mL of distilled $HNO_3$ to break up insoluble fluoride salt that may have formed during the sample digestion and $HNO_3$ was left to evaporate at 110 °C. This step was repeated twice before weighing the sample and adding 5 mL of 2% $HNO_3$. The sample was sonicated for 10 min in a sonication bath (Branson, 2800, 40 kHz, Mexico) and warmed for 2 h at 50 °C for full dissolution. The solution was transferred to 15 mL polypropylene centrifuge tubes (Eppendorf, Mexico) and stored at 4 °C. Samples were centrifuged (Eppendorf, 5810 R, Germany) for 5 min at 3100 g prior ICP-MS analysis to remove any undigested minerals.

Elemental concentrations of the digested water samples were analyzed by high resolution ICP-MS (ThermoFisher Element II, USA) (Frisby et al., 2016). Samples were injected to the ICP-MS using a quartz cyclonic spray chamber and a 100 μl $min^{-1}$ PFA nebulizer (~120–-150 μL $min^{-1}$ actual uptake). The isotopes measured were $^{57}Fe$, $^{107}Ag$, $^{139}La$ and $^{140}Ce$. Elements with potential interferences (*e.g.*, Fe) was measured in medium resolution ($m/\Delta m = 4000$), while the rest in low resolution for maximum sensitivity ($m/\Delta m = 300$). Concentrations were calculated against a multi-element standard solution composed of a mixture of IV-ICP-MS-71A (ICP-MS Complete Standard, Inorganic Ventures, USA) and ICP-MS-68A-B (68 Element Standard, High-Purity Standards, USA) multi-element standards.

Full procedural digestion blanks for Fe, Ag, Ce and La averaged 4% of the analyte signal. Therefore, blanks are insignificant to the calculations of elemental concentrations or elemental ratios. The elemental concentrations of the USGS reference materials BCR-2 and BIR-1 basalts run as unknowns after digestion following the digestion procedure described above demonstrate high recovery (approximately 100%) for most elements, with a precision of 2–3% and accuracy better than 5% for most elements.

### 2.7. Estimation of ENM concentration in the extracted suspensions

Due to the low concentration of naturally occurring Ag, the concentration of Ag due to the presence of ENMs in the extracted 100 and 450 nm suspensions was estimated according to Eq. (1)

$$[Ag]_{ENMs} = [Ag]_{sample} - [Ag]_{background} \quad (1)$$

where, $[Ag]_{background}$ represents the concentration of silver in the river water without ENM spike.

Due to the occurrence of $CeO_2$ as NNMs, the concentration of $CeO_2$ ENMs in the extracted suspensions according to Eq. (2)

$$[CeO_2]_{ENMs} = \frac{CeO_{2MM}}{Ce_{MM}}\left[Ce_{sample} - La_{sample}\cdot\left(\frac{Ce}{La}\right)_{background}\right] \quad (2)$$

where, $[CeO_2]_{ENMs}$ is the concentration of $CeO_2$ engineered nanoparticles, $Ce_{MM}$ and $CeO_{2\ MM}$ are the molar masses of Ce and $CeO_2$, Ce/La is the mass ratio of Ce to La. Background Ce/La ratios were calculated as the average of the 0.05 μg $L^{-1}$ $CeO_2$ spiked sample extracted with 0.5 mM NaOH and no ENM doping for the extraction with 10 mM $Na_4P_2O_7$.

### 2.8. Size-based elemental distributions of the extracted suspensions: AF4-ICP-MS

Size based elemental distribution of the <0.1 μm extracted suspensions (see Section 2.5) from the ENM-spiked river water was determined by AF4-ICP-MS. AF4-ICP-MS was performed by coupling Wyatt AF4 (DualTec Eclipse, Wyatt Technology, USA) with a NexION350D (Perkin Elmer, USA). All separation experiments on AF4 used a 10 kDa molecular weight cut-off regenerate cellulose membrane (Superon, Germany) and 350 μm spacer. Carrier solution used in AF4 channel was composed 10 mM $NaNO_3$ (VWR Analytical, BDH®, ACS, Canada), 0.01% sodium azide (Fisher Chemical, India) and 0.0125% FL-70 (Fisher Chemical, USA) in UPW. Samples injection volumes were 900 μL with 10 min focus time. The detector flow was set to 1.0 mL $min^{-1}$ and a constant cross flow of 1 mL $min^{-1}$ was applied. The elution time was set to 50 min for the water samples. Latex Nanosphere Size Standards (Thermo Scientific, USA) in sizes of 20, 40, 80, and 150 nm were used to calibrate particle size *vs.* elution time under the same experimental conditions.

Multi-element standards mixture of IV-ICP-MS-71A (ICP-MS Complete Standard, Inorganic Ventures) and ICP-MS-68A-B (68 Element Standard, High-Purity Standards) diluted in 1% $HNO_3$ (Trace Metal grade, Fisher Chemical, USA) were used for mass concentration calibration ranging from 0.01 to 100 μg $L^{-1}$ before coupling. Internal standard (ICP Internal Element Group Calibration Standard, BDH Chemicals, USA) was monitored at the same time for quality control. A 50 ms dwell time for all the analytes was applied. Chromera 4.1.0.6386 were utilized to collect AF4-ICP-MS data. A 20 min 1% $HNO_3$, a 20 min 2% methanol rinse and a 10 min UPW rinse were applied field-off between each sample.

### 2.9. Number size distribution: sp-ICP-MS

Single particle ICP-MS data was collected for Ag ENMs on Perkin Elmer NexION350D using Syngistix 1.0 data processing software. A 50 μs dwell time was utilized with acquisition time of 60 s. Transport efficiency was determined by particle size with National Institute of Standards and Technology (NIST, USA) 60 nm Au ENMs (RM 8013) following the method previously described by Pace et al. (2011). Dissolved gold standards concentrations range from 0 to 20 μg $L^{-1}$, prepared in 1% hydrochloric acid (HCl, Trace Metal grade, Fisher Chemical, USA). Dissolved silver standards were prepared in 1% $HNO_3$, with same concentration range as dissolved gold.

### 2.10. Transmission electron microscopy

Size distribution analysis of Ag ENMs was performed using transmission electron microscope (TEM). TEM samples were prepared using drop deposition method according to the procedure described elsewhere (Prasad et al., 2015). Briefly, TEM grids were functionalized using a positively charged poly-L-lysine (1% *w/v* in water solution; Ted Pella, USA) to enhance the attachment of the negatively charged Ag ENMs on the grid surface. 10 μL of poly-L-lysine were deposited on a 300 mesh Cu grid (Ted Pella, Pelco®, USA) for 20 min followed by rinsing three consecutive times in UPW water to remove excess poly-L-lysine. Subsequently, 20 μL of Ag ENM stock suspension were deposited on the functionalized TEM grids for 15 min. The excess Ag ENM suspension was then removed by immersing the TEM grid three times in UPW to avoid ENM aggregation during the drying process. The TEM grids were then left to dry for 12 h in a covered petri dish to avoid atmospheric particle deposition on the TEM grid. Samples were analyzed in a $LaB_6$ Jeol 2100 TEM, operated at 200 keV. The particle diameter was determined using image J on 165 individual particles, which were used to construct the particle size distribution histogram and to determine the mean diameter and standard deviation of the size distribution, where the standard deviation represents the width of the size distribution.

## 3. Results and discussion

### 3.1. Physicochemical properties of Ag, $Fe_2O_3$, and $CeO_2$ ENMs

The core diameter of Ag ENMs in stock suspension was determined by transmission electron microscope (TEM) and single particle-inductively coupled plasma-mass spectrometer (sp-ICP-MS), and the z-average hydrodynamic diameter was determined by dynamic light scattering (DLS). TEM micrograph shows that Ag ENMs are spherical with most of the particles occurring as individual particles with few aggregated particles (Fig. 1a). The number particle size distribution of Ag ENMs measured by TEM (Fig. 1b) shows that the size of primary Ag ENMs varies between 3 and 20 nm, for the 160 particles analyzed, with the majority (*e.g.,* 61%) of Ag ENMs being smaller than 7 nm and with a tailing toward larger sizes. The mass-based particle size distribution, calculated by converting the number-based particle size distribution measured by TEM to mass-based size distribution, show a bimodal mass-based size distribution of Ag ENMs with a peak of small Ag ENMs centered at 8–9 nm and a peak of larger Ag ENMs centered at 17–18 nm. The mean number- and mass- equivalent circular diameters of Ag ENMs determined by TEM were 6.7 ± 3.3 nm and 11.7 ± 4.1 nm, respectively. The number particle size distribution of Ag ENMs, measured by sp-ICP-MS (Fig. 1c), displays a monomodal particle size distribution centered at 24 nm. The number mean equivalent spherical diameter determined by sp-ICP-MS was 23.1 ± 3.7 nm. The larger number mean size determined by sp-ICP-MS compared to the number mean size determined by TEM is due to the size detection limit of sp-ICP-MS (Lee et al., 2014); that is 18 nm for the sp-ICP-MS configuration used in this study. Thus, Ag ENMs <18 nm in diameter were not measured by sp-ICP-MS, resulting in a bias of the sp-ICP-MS determined number size distribution toward larger particle sizes relative to the TEM determined number size distribution. The z-average hydrodynamic diameter, polydispersity index, and the zeta potential of Ag ENMs in the stock suspension (*e.g.,* in 0.26 mM sodium citrate at pH 7) were 22.4 ± 0.3 nm, 0.15, and −42.8 ± 1.3 mV, respectively. The z-average hydrodynamic diameter of Ag ENMs was greater than the number mean diameter determined by TEM, but it was in good agreement with the number mean diameter determined by sp-ICP-MS. These differences are attributed to the differences in the measurement principles of the different techniques, the weighting of the size distribution, and the determined size measured as discussed elsewhere (Baalousha and Lead, 2012). Briefly, DLS measures the intensity-weighted hydrodynamic diameter, which is typically larger than the number-weighted core diameter measured by TEM, except for highly monodispersed ENMs (*e.g.,* PDI < 0.05) (Baalousha and Lead, 2012). The good agreement between intensity-weighted z-average hydrodynamic diameter and the number-weighted core diameter measured by TEM is rather unexpected, but can be attributed to the bias in the number-weighted

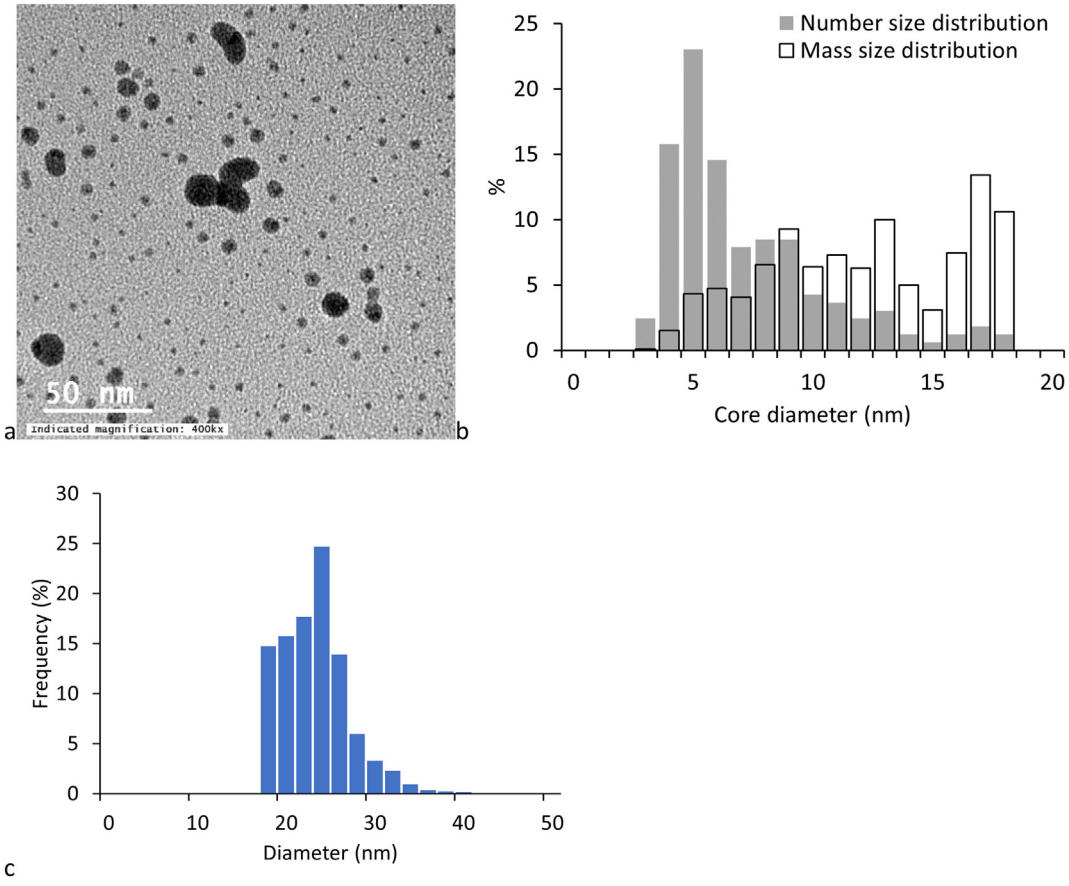


**Fig. 1.** (a) Transmission electron microscopy (TEM) micrograph and (b) particle size distribution of Ag ENMs based on TEM micrograph analysis of 160 particles, and (c) number particle size distribution measured by single particle-inductively coupled plasma-mass spectroscopy (sp-ICP-MS) of 5500 particles.

measured core diameter by sp-ICP-MS toward larger values due to the sp-ICP-MS detection limit of 18 nm for Ag ENMs.

The primary number mean core diameter of $CeO_2$ ENMs in the stock suspension, measured by scanning electron microscopy (SEM), was 28.4 ± 10.4 nm (Singh et al., 2014). The z-average hydrodynamic diameter of $CeO_2$ ENMs in the stock suspensions was 325 ± 77 nm and decreased to 214 ± 8 in 0.5 mM NaOH at pH 10. The primary particle core diameter of $Fe_2O_3$ ENMs, determined by Brunauer-Emmett-Teller (BET) surface area analyzer, according to the supplier information was <50 nm. The z-average hydrodynamic diameter of $Fe_2O_3$ ENMs in the stock suspensions was 305 ± 60 nm decreased to 230 ± 10 in 0.5 mM NaOH at pH 10. The larger z-average hydrodynamic diameters of $CeO_2$ and $Fe_2O_3$ ENMs in the stock suspensions compared to their primary particle size suggest that they readily formed aggregates in the stock suspensions as demonstrated previously in numerous studies (Baalousha et al., 2012; Domingos et al., 2009). The smaller z-average hydrodynamic diameters at pH 10 compared to those measured in the stock suspension suggest that raising the suspension pH break $CeO_2$, and $Fe_2O_3$ ENM aggregates into smaller aggregates, but does not fully break them down to primary particles (Loosli et al., 2018).

### *3.2. Evaluation of sample preparation for measurement of ENM concentration by ICP-OES*

Fig. 2 shows the total concentration of ENMs measured by ICP-OES following different sample preparation procedure (*e.g.,* dilution in UPW, acidification by $HNO_3$, and HF digestion) normalized by the nominal ENMs concentrations in the samples. HF digestion resulted in measuring 99.9 ± 0.9%, 80.1 ± 3.1%, and 82.4 ± 4.0% of nominal concentrations of Ag, $CeO_2$, and $Fe_2O_3$ ENMs, respectively. The high recovery of Ag ENMs is likely due to their high stability and thus the homogeneity of the sample, reducing any error during sample preparation (*e.g.,* pipetting, dilution and digestion). The lower recovery of $CeO_2$ and $Fe_2O_3$ ENMs compared to Ag ENMs might be attributed to losses of $CeO_2$ and $Fe_2O_3$ ENMs during sample preparation (*e.g.,* pipetting, weighting, and dilution, and digestion), or to the inhomogeneity in the $CeO_2$ and $Fe_2O_3$ ENM suspensions due to their aggregation. Thus, the measured rather than nominal concentrations of Ag, $CeO_2$, and $Fe_2O_3$ ENMs are reported in all results below to avoid misrepresentation of the actual experimental concentrations, which could be lower than

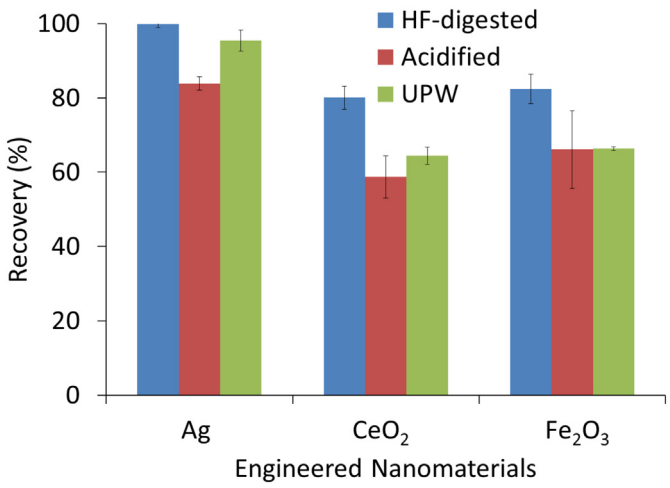


**Fig. 2.** Recovery (%) of the measured ENM concentrations compared to nominal concentrations. All elemental analyses were performed using inductively coupled plasma-optical emission spectroscopy (ICP-OES).

the nominal concentrations due to sample losses during sample preparation (*e.g.*, pipetting, weighting and dilutions). The concentration of ENMs measured with acidification using 2% $HNO_3$ or without acidification using UPW were slightly lower than those measured following HF digested. Acidification using $HNO_3$ resulted in measuring 83.9 ± 1.8%, 58.7 ± 5.7%, and 66.1 ± 10.4% of nominal concentrations of Ag, $CeO_2$, and $Fe_2O_3$ ENMs, respectively. The measured ENM concentrations following dilution in UPW were 95.4 ± 2.9%, 64.4 ± 2.3%, and 66.3 ± 0.6% of nominal concentrations of Ag, $CeO_2$, and $Fe_2O_3$ ENMs, respectively. Thus, HF digestion is recommended prior to ICP-OES and ICP-MS analysis to ensure a correct quantification of the total metal concentration. These findings are in agreement with previous studies demonstrating that acid digestion is a more accurate compared to acidification and dilution in UPW for total elemental analysis (Fabricius et al., 2014).

### 3.3. Extraction of ENMs in synthetic soft water

The % of the extracted Ag ENMs, in comparison to the amount of the spiked ENM (50 μg $L^{-1}$), in the <450 nm and < 100 nm size fractions were 77.6–101.1% for all extraction procedures (Fig. 3). Ag ENMs used in this study were lab synthesized small ENMs with a z-average hydrodynamic diameter of approximately 22.4 ± 0.3 nm and a high zeta potential of −42.8 ± 1.3 mV (See Section 3.1). The high recovery of Ag ENMs in the <450 and < 100 nm size fractions indicates their stability and thus homogeneity in synthetic soft water. For the 0.5 mM NaOH extraction, the slightly low % Ag ENMs in the <450 nm and < 100 nm (*ca.* 93 ± 1.9 and 86 ± 4.9, respectively) in synthetic soft water is likely due to the slight aggregation of Ag ENMs. Although soft water is a low ionic strength media, the concentration of divalent counter ions in the synthetic soft water is 0.6 mM, which may result in the aggregation of Ag ENMs in reaction limited aggregation regime and thus the formation of small Ag ENM aggregates (Baalousha et al., 2013), which may be removed during the filtration process. For the oxalate ($Na_2C_2O_4$) extraction, the % Ag ENMs in the <450 nm and < 100 nm fractions were either not statistically different or slightly lower, at 10 mM $Na_2C_2O_4$, than the corresponding % Ag ENMs in the corresponding fractions in the 0.5 mM NaOH-extracted suspensions. For the pyrophosphate ($Na_4P_2O_7$) extraction, the % Ag ENMs in in the <450 and < 100 nm fractions were either not statistically different or slightly higher than the % Ag ENMs in the corresponding fractions in the 0.5 mM NaOH-extracted suspensions and higher than those measured in the $Na_2C_2O_4$ extraction. $Na_2C_2O_4$ enhances the aggregation of Ag ENMs in particular at high $Na_2C_2O_4$ concentrations; whereas, $Na_4P_2O_7$ enhances the stability of Ag ENMs by enhancing ENM surface charge and sequestering divalent cations from the suspension (Loosli et al., 2018).

The %, $CeO_2$ and, $Fe_2O_3$ ENMs in 0.5 mM NaOH-extracted suspensions were 74.2 ± 3.7 and 50.3 ± 14.1% in the fraction <450 nm and 34.6 ± 3.4 and 8.3 ± 1.1% in the fraction <100 nm, indicating the poor extraction of these ENMs using 0.5 mM NaOH due to their aggregation in synthetic soft water, even in the presence of 5 mg $L^{-1}$ SRHA (Oriekhova and Stoll, 2016; Ramirez et al., 2019). $CeO_2$ and $Fe_2O_3$ ENMs used in this study are commercially available powders which readily form aggregates when suspended in UPW as discussed above (Loosli et al., 2018; Rasmussen et al., 2014; Singh et al., 2014). For the $Na_2C_2O_4$ extraction, the % ENM concentrations remained nearly constant at 2 mM $Na_2C_2O_4$ and decreased at 10 mM $Na_2C_2O_4$ compared to those measured in the 0.5 mM NaOH-extracted suspensions (Fig. 3a and b). $Na_2C_2O_4$ has been shown to induce ENM (*e.g.*, $TiO_2$ and other) aggregation and to be insufficient to break clay-ENM heteroaggregates (Loosli et al., 2018). The lower % ENM extracted at higher $Na_2C_2O_4$ concentration, except for the <100 nm $Fe_2O_3$, which remained constant with the increase in $Na_2C_2O_4$ concentration, is likely due to the increased ENM aggregation with the increase in $Na_2C_2O_4$ concentration.

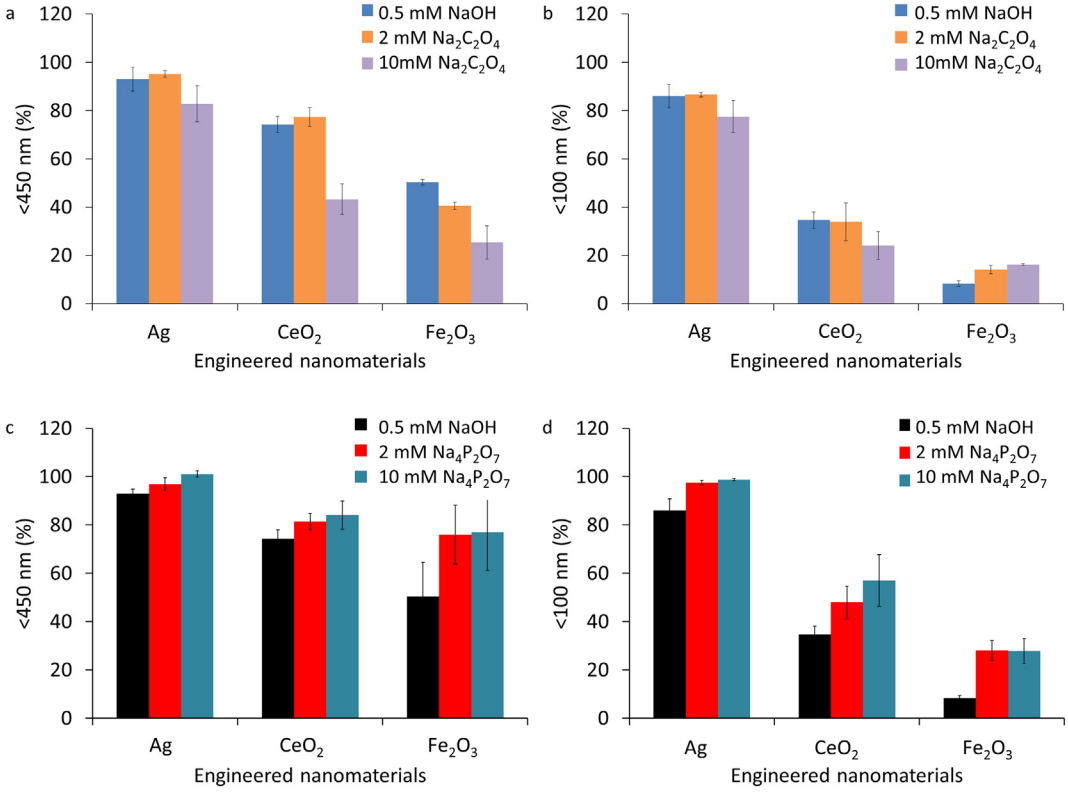


**Fig. 3.** Concentration (%) of extracted Ag, $CeO_2$ and $Fe_2O_3$ ENMs from a synthetic soft water containing 5 mg $L^{-1}$ Suwannee River humic acid (SRHA)-spiked with ENMs (50 μg $L^{-1}$ of Ag, Ce and Fe, respectively) compared to their corresponding total concentration spiked in the soft water as a function of extraction treatment and extracted ENM size cutoff: (a) oxalate ($Na_2C_2O_4$)-extracted ENMs <450 nm, (b) $Na_2C_2O_4$-extracted ENMs <100 nm, (c) pyrophosphate($Na_4P_2O_7$)-extracted ENMs <450 nm, and (d) $Na_4P_2O_7$-extracted ENMs <100 nm. All elemental analyses were performed using inductively coupled plasma-optical emission spectroscopy (ICP-OES).

For $Na_4P_2O_7$ extraction, the % ENM concentrations in the <450 nm and < 100 nm fractions were significantly higher than those measured in the corresponding size fraction in the 0.5 mM NaOH-extracted suspensions. Pyrophosphate sorbs on the surfaces of ENMs and enhances the breakup of ENM aggregates into smaller aggregates and/or primary ENMs. For a given ENM, the % ENM concentrations in the <450 nm fraction was significantly higher than those in the <100 nm fraction, suggesting that a significant fraction (*e.g.*, 30–50%) of ENM aggregates occur in the size range 100–450 nm. The % of ENM in the <450 nm (Fig. 3a *vs.* c) and < 100 nm (Fig. 3b *vs.* d) fractions are higher in the $Na_4P_2O_7$-extracted EMMs compared to the $Na_2C_2O_4$-extracted ENMs indicating the higher efficiency of $Na_4P_2O_7$ to break ENM aggregates to smaller sizes. Thus, $Na_4P_2O_7$ is more suitable to extract ENMs than $Na_2C_2O_4$. Nonetheless, disaggregation of ENM – particularly commercial powder-type ENMs – into their primary particles (*e.g.*, < 100 nm) remains challenging due to the strong interaction forces between the primary ENMs (Taurozzi et al., 2012). It is therefore critical to consider ENM aggregation behavior when measuring total ENM concentration in environmental systems as the majority of ENMs form aggregates in natural systems. Thus, the <100 nm size fraction – even with the most efficient extraction protocol – is likely to represent only a small fraction of the total ENM concentration in any environmental system.

### 3.4. Extraction of ENMs from spiked river water

The concentrations of Ag, Ce, and Fe, used as a proxy for Ag and $CeO_2$ and $Fe_2O_3$ ENMs, in the extracted suspensions from ENM-spiked river water are presented in Fig. 4. The concentration of Ag and Ce in the dissolved fraction for both 0.5 mM NaOH and 10 mM $Na_4P_2O_7$-extractions were < 0.1 and 0.15 μg $L^{-1}$ for all extractions and for all spiked ENM concentrations indicating that the large majority of Ag and Ce were extracted in the form of NMs and that $Na_4P_2O_7$ did not increase the dissolution of Ag and $CeO_2$ ENMs within the extraction time used in this study. The concentration of Fe in the dissolved fraction in the 0.5 mM NaOH extracted suspension was <2.7 μg $L^{-1}$ and in the $Na_4P_2O_7$-extracted suspensions was 74–80 μg $L^{-1}$ indicating that $Na_2P_4O_7$ results in the extraction of high concentrations of dissolved Fe and/or the dissolution of iron oxide particles (ENMs and NNMs). Regelink et al., reported the formation of metal (*e.g.* iron)-pyrophosphate complexes during iron based NM extraction from soils using $Na_4P_2O_7$ with a significative formation of polymeric-iron complexes eluting at the beginning (*e.g.*, corresponding to <1.6 kDa cutoff) of the AF4 run (Regelink et al., 2013).

The concentration of Ag in the extracted suspensions was below or close to the detection limit (*e.g.*, 15 ng $L^{-1}$) for the 0.05, 0.5, and 5 μg $L^{-1}$ ENM spiked river water samples, possibly due to the heteroaggregation of Ag ENMs with natural particles and their removal during the filtration process (Wang et al., 2015). For the 50 μg $L^{-1}$ ENM spiked river water samples, the concentration of Ag in the extracted suspensions was not higher and/or even lower in the <450 nm fraction than in the <100 nm fraction. Similar Ag concentrations in both size fractions may be due to the narrow size distribution of the Ag ENMs with particle sizes being smaller than 100 nm (Fig. 1) whereas the slightly higher Ag ENM concentration in the <100 nm fraction, for $Na_4P_2O_7$ -extracted suspensions, may arise from the non-homogeneity and high polydispersity of the size of natural colloids and other particulate matters in natural waters (Baalousha et al., 2006). Indeed, some of the heteroaggregates formed between Ag ENMs and natural particulate matters will be removed during filtration processes and higher proportion (*e.g.*, >80%) of Ag ENMs form heteroaggregates with sizes larger than the first filtration membrane pore size (*e.g.* >450 nm). The concentration of dissolved Ag (*e.g.* <3 kDa) represents <0.2% of the 50 μg $L^{-1}$ spiked Ag which is in good agreement with a previous study which investigated the dissolution of citrate-coated Ag NM in natural waters (Li and Lenhart, 2012). The concentration of Ce was generally higher in the <450 nm fraction than in the <100 nm fraction which can be attributed to the broader size distribution and higher mode value for $CeO_2$ ENMs than for Ag ENMs. This results in the removal of an additional fraction

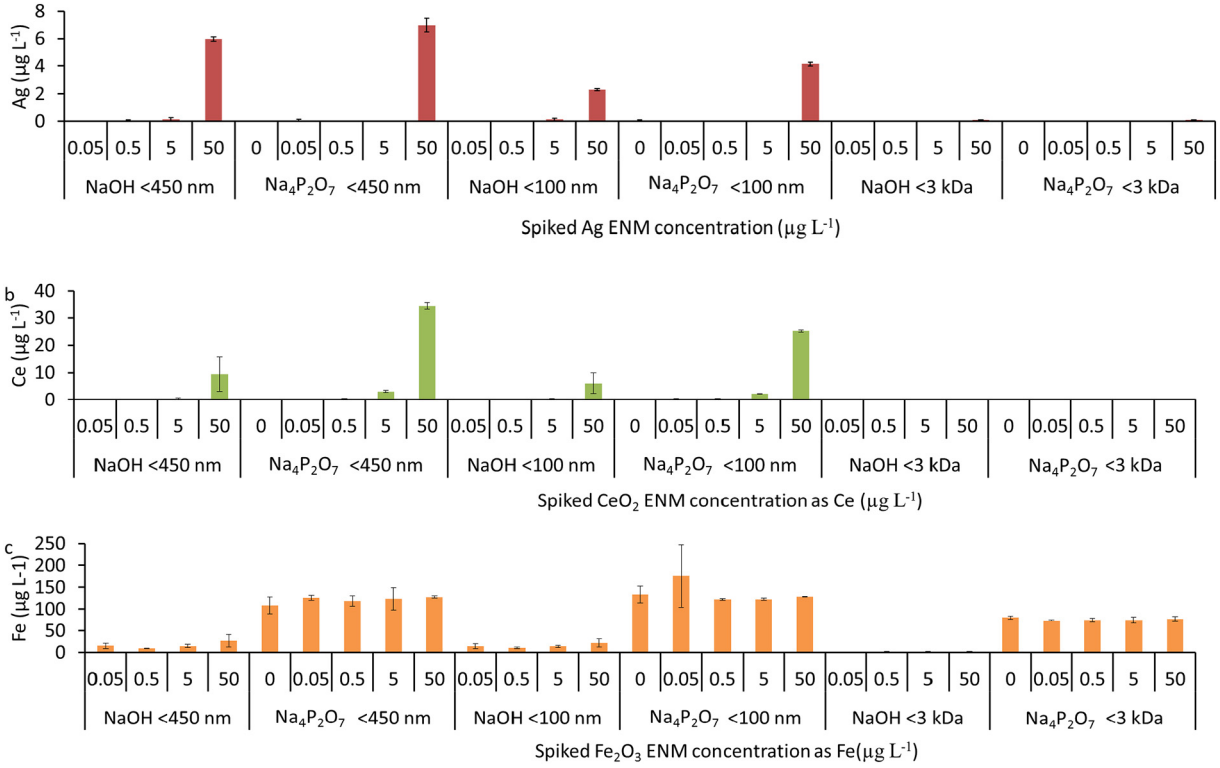


**Fig. 4.** Concentration of Ag, Ce and Fe in the extracted colloidal (<450 nm), nano (<100 nm) and dissolved (<3 kDa) fractions as a function of spiked ENM (0–50 μg $L^{-1}$, upper number value) concentrations for (a) Ag and (b) Ce (as $CeO_2$ ENM) and (c) Fe (as $Fe_2O_3$ ENM). NMs were separated by filtration over 450, 100 nm and 3 kDa membranes. All elemental analyses were performed using inductively coupled plasma-mass spectroscopy (ICP-MS).

of $CeO_2$ ENMs during the second separation process (filtration <100 nm). The concentration of Ce in the $Na_4P_2O_7$-extracted suspensions from ENM-spiked river water are generally higher than those in the unspiked river water sample for both the <100 and < 450 nm size fractions. Additionally, the concentrations of $CeO_2$ ENMs extracted in both size fractions using 10 mM $Na_4P_2O_7$ is the same as the concentrations of $CeO_2$ ENMs extracted in the synthetic soft waters (*e.g.*, 80 and 60% for the <450 and <100 nm fractions, respectively). The similar recovery of $CeO_2$ ENMs in $Na_4P_2O_7$ for both river and synthetic water may be attributed to the lower binding energy between $CeO_2$ ENMs and natural colloids and/or higher affinity of pyrophosphate for $CeO_2$ in comparison to Ag ENMs. These results indicate that $CeO_2$ ENMs were likely extracted as a mixture of primary ENMs and aggregates of ENMs. $Na_4P_2O_7$ braks ENM-natural particle heteroaggregates (Loosli et al., 2019b) into smaller aggregates and/or into primary particles; thus, the higher concentrations of ENMs in the $Na_4P_2O_7$-extracted suspensions. The concentrations of Fe in the $Na_4P_2O_7$ extracted suspensions were higher than those in the 0.5 mM NaOH extracted concentrations. However, the concentrations of Fe in the extracted suspensions did not show any trend with the increase in the spiked $Fe_2O_3$ ENM concentrations. This is likely due to the high concentration of iron oxide NNMs in surface waters, which dominates the relatively low spiked $Fe_2O_3$ ENM concentrations. The detectability and quantification of $Fe_2O_3$ ENMs in the river water, under the present experimental conditions, were thus not enhanced by the $Na_4P_2O_7$ extraction.

### *3.5. Concentration of Ag and $CeO_2$ engineered nanomaterials in the river water*

The concentration of Ag in the unspiked river water sample was below the detection limit. The dissolved Ag in the river water from Ag ENMs represents a small fraction (*e.g.*, < 0.2 wt%) of the total spiked Ag ENM concentrations (Fig. 4a). Thus, the measured Ag concentrations can be used as a direct measure of Ag ENM concentrations in the river water. The Ag ENM recovery was generally low and varied between 5 and 15%.

The concentration of Ce in the extracted river water sample in the absence of spiked ENMs were low (*e.g.*, < 0.15 μg $L^{-1}$). Thus, the measured Ce concentrations in the ENM-spiked river waters can be attributed to $CeO_2$ ENMs. Nonetheless, as a proof of concept to the application of the Ce/La elemental ratios to calculate $CeO_2$ ENM concentrations, the Ce/La ratio was calculated as a function of the spiked ENM concentrations to evaluate the possibility of detecting $CeO_2$ ENMs in river water based on the increase in Ce/La ratio due to the introduction of pure $CeO_2$ ENMs. The Ce/La in the extracted suspensions increased with the increase in the spiked-$CeO_2$ ENM concentration (Fig. 5a) for both NaOH- and $Na_4P_2O_7$-extracted suspensions, indicating the increase in the concentration of extracted $CeO_2$ ENMs with the increase in the spiked $CeO_2$ ENM concentrations. The Ce/La ratio was lower in the $Na_4P_2O_7$-extracted suspensions than in the NaOH-extracted suspensions, likely due to the extraction of higher concentration of $CeO_2$

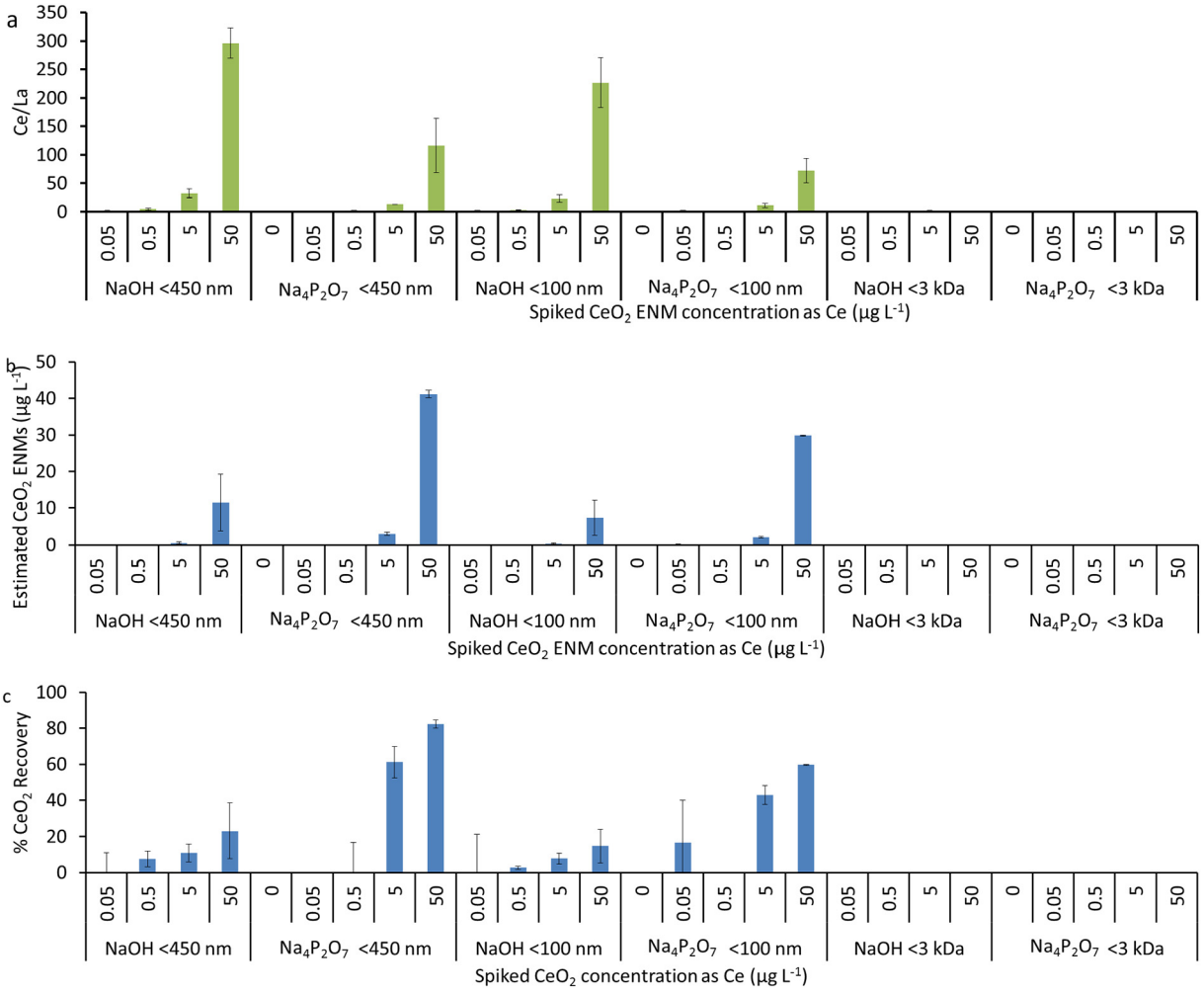


**Fig. 5.** (a) Ce/La elemental ratio for the extracted fractions, (b) the calculated $CeO_2$ concentrations in the river water using elemental ratios and total Ce concentration, and (c) the % recovery of $CeO_2$ ENMs from surface water spiked with $CeO_2$ ENMs. The baseline Ce/La of the unspiked water sample was used as the baseline to estimate $CeO_2$ ENM concentrations.

NNMs. Nonetheless, the concentration of $CeO_2$ ENMs in the pyrophosphate-extracted suspensions was higher than those measured in the 0.5 mM NaOH-extracted suspensions (Fig. 5b) for both the <450 and < 100 nm extracted suspensions.

The $CeO_2$ ENM concentration in the extracted <450 nm suspensions is higher than those in the extracted <100 nm suspensions (Fig. 5c). The $CeO_2$ ENM concentrations in the $Na_4P_2O_7$-extracted <450 nm and < 100 nm fractions represent approximately 80% and 60% of the total spiked $CeO_2$ ENM concentrations at the highest spiked $CeO_2$ ENM concentration. The $CeO_2$ ENM recovery is lower at lower spiked ENM concentrations, which might be due to the lower elemental ratios, and thus the higher error in estimating $CeO_2$ ENM concentrations based on elemental ratios at low $CeO_2$ ENM concentrations. These results suggest that the majority of the extracted $CeO_2$ ENMs occurred in sizes <100 nm and that only 20% of the $CeO_2$ occurred as aggregates >450 nm in size. The higher recovery of $CeO_2$ ENMs (*e.g.*, 40–60%) than that of Ag ENMs (*e.g.*, 5–15%) might be attributed to the higher affinity of pyrophosphate to $CeO_2$ than Ag ENMs.

### *3.6. Size distribution of engineered nanomaterials extracted from river water*

Fig. 6a-b shows Ag and $CeO_2$ ENM size distributions of the <100 nm $Na_4P_2O_7$ extracted suspensions measured by AF4-ICP-MS. The size distribution of Ag ENMs ranges from 0 to 60 nm with a bimodal size distribution with a first peak centered at 6 nm and a second peak centered at 17 nm. These sizes are in good agreement with the mass-based primary particle size distribution of Ag ENMs calculated from the number-based size distribution determined by TEM (Fig. 1), suggesting that the size distribution of extracted Ag ENMs is representative of the original Ag ENMs. Higher concentration of Ag ENMs in the $Na_4P_2O_7$-extracted suspensions in comparison to NaOH-extracted suspensions (SI, **Fig. S1a**) indicates the higher recovery of Ag ENMs in presence of $Na_4P_2O_7$, in good agreement with the total metal concentration data presented above (Fig. 4a).

The concentration of Ce in the 0.5 mM NaOH-extracted NMs was very low and was not detectable by AF4-ICP-MS (SI, **Fig. S1b**). The concentration of Ce in the $Na_4P_2O_7$-extracted suspensions (Fig. 6b) was generally higher than those measured in 0.5 mM NaOH-extracted suspensions and increased with the increase in the spiked $CeO_2$ ENM concentrations in good agreement with the increase in the total $CeO_2$ ENM concentration measured by total digestion (Fig. 5c). The cerium and lanthanum concentrations were very low in the 0.5 mM NaOH-extracted suspensions, and thus it was not possible to calculate the Ce/La ratio (SI, **Fig. S1c**). For $Na_4P_2O_7$-extracted suspensions, the Ce/La ratio (Fig. 6c) increased with the increase in the spiked $CeO_2$ ENM concentrations, a clear indication of the increased concentration of $CeO_2$ ENMs in the extracted suspensions. The size distribution of $CeO_2$ ENMs varied between 10 and 200 nm with 70.5% of the $CeO_2$ particles in the size range < 100 nm, indicating that the extracted $CeO_2$ ENMs were a mixture of primary ENMs and homo/heteroaggregates of $CeO_2$ ENMs, further confirm that $Na_4P_2O_7$ improves the dispersion of $CeO_2$ ENMs.

The number size distributions of Ag ENMs extracted from River water using 0.5 mM NaOH and 10 mM $Na_4P_2O_7$ measured by sp-ICP-MS are presented in Fig. 7. The number size distribution of the extracted Ag ENMs is similar to that of the Ag ENM stock suspension (Fig. 1c). The mean number size of Ag ENMs was 28 ± 5 nm and 25 ± 4 for the 0.5 mM NaOH and 10 mM $Na_4P_2O_7$-extracted ENMs. The mean sizes measured by sp-ICP-MS are larger than those measured by AF4-ICP-MS, which can be attributed to the sp-ICP-MS detection limit of 18 nm for Ag ENMs. The mean size of Ag ENMs is very close to the size detection limit of Ag ENMs by sp-ICP-MS and the size distribution shows a non-Gaussian distribution indicating that some small Ag ENMs were possibly measured as dissolved ions. Thus, the mean sizes reported here are higher than the actual (measured by TEM) mean size of Ag ENMs.

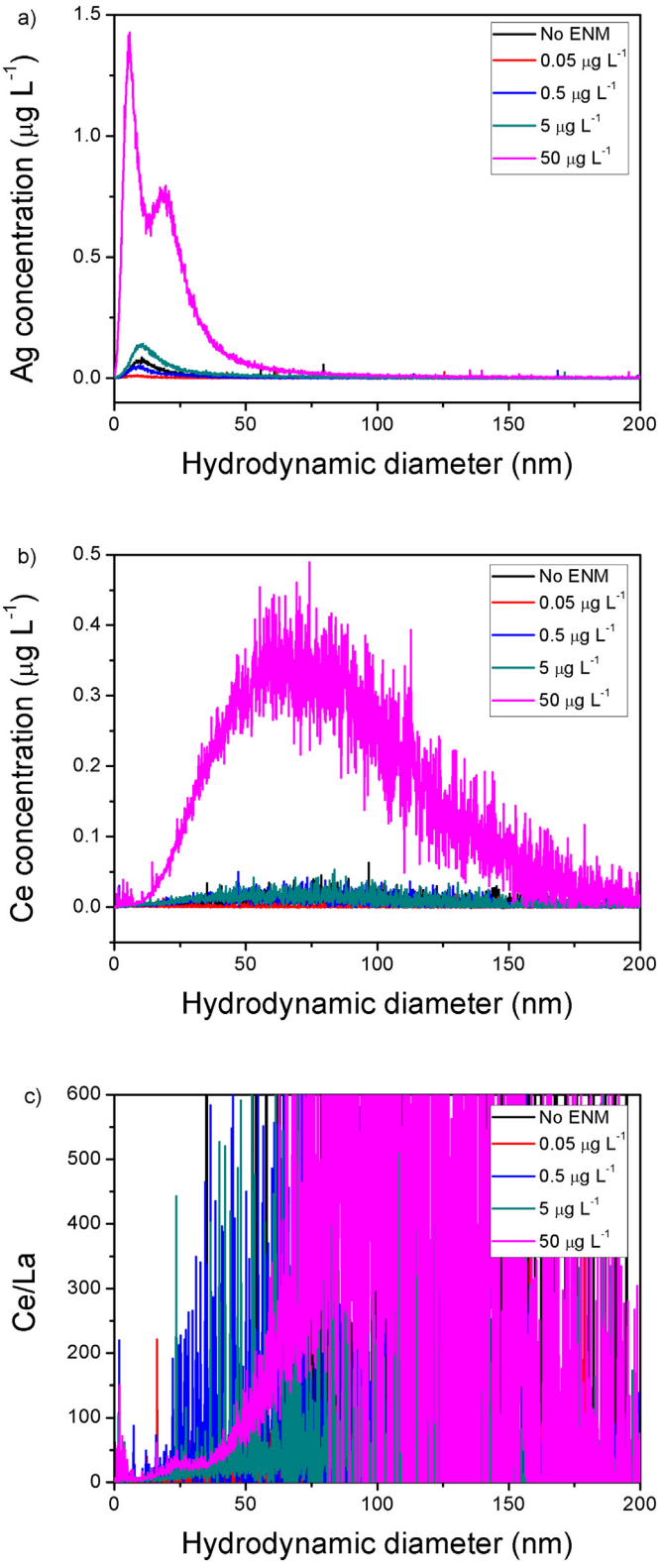


**Fig. 6.** Size-based hydrodynamic diameter of the <100 nm $Na_4P_2O_7$-extracted suspensions from ENM-spiked river waters for (a) Ag, (b) Ce and (c) Ce/La elemental ratios.

## 4. Conclusions

This study presents a protocol to extract ENMs from surface water-spiked with ENMs, which can be applied to analyze ENMs in natural environmental samples. The $Na_4P_2O_7$ extraction resulted in higher recovery of Ag and $CeO_2$ ENMs than that obtained for the 0.5 mM NaOH

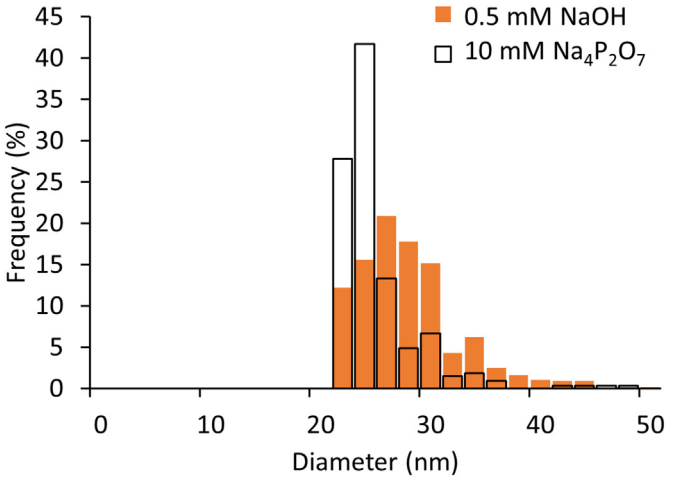


**Fig. 7.** Number particle size distribution of the Ag ENMs extracted from ENM-spiked river waters using 0.5 mM NaOH and 10 mM $Na_4P_2O_7$. The number particle size distribution was measured by SP-ICP-MS. Ag ENM concentration was 5 μg $L^{-1}$.

extraction, due to the higher efficiency of $Na_4P_2O_7$ to break up natural and engineered NM heteroaggregates. The concentration $CeO_2$ ENMs were generally higher in the colloidal fraction (< 450 nm) compared to the nanofraction (< 100 nm). This indicates the extraction of $CeO_2$ ENMs as primary particles and as small heteroaggregates. Ag ENMs were also extracted as a mixture of both primary particles and aggregates but Ag concentrations remain similar in both the <450 nm and < 100 nm size fractions. The size distribution of the extracted ENMs was measured by AF4-ICP-MS and sp-ICP-MS. The size distribution of extracted Ag ENMs was in agreement with their corresponding size distribution in the stock suspension and confirms that the extracted Ag ENMs were a mixture of primary and small aggregates. The size distribution of the extracted $CeO_2$ ENMs ranged from 0 to 200 nm. The advantage of AF4-ICP-MS compared to sp-ICP-MS was in measuring the smaller Ag ENMs (*ca.* < 18 nm), which were not detected by sp-ICP-MS due to the size detection limit of sp-ICP-MS. Thus, AF4-ICP-MS fills a major gap for the detection of small ENMs and is a method of choice to complement the ENM characterization in complex environmental samples in addition to sp-ICP-MS and total digestion analyses.

## Acknowledgment

This work was supported by US National Science Foundation CAREER (1553909) grant to Dr. Mohammed Baalousha, Swiss National Science Foundation postdoctoral mobility funding (P2GEP2_165046) to Dr. Frederic Loosli. This work was supported by the Virginia Tech National Center for Earth and Environmental Nanotechnology Infrastructure (NanoEarth), a member of the National Nanotechnology Coordinated Infrastructure (NNCI), supported by NSF (ECCS 1542100).

## Appendix A. Supplementary data

Supplementary data to this article can be found online at https://doi.org/10.1016/j.scitotenv.2020.136927.

## References

Baalousha, M., Lead, J.R., 2012. Rationalizing nanomaterial sizes measured by atomic force microscopy, flow field-flow fractionation, and dynamic light scattering: sample preparation, polydispersity, and particle structure. Environ Sci Technol 46, 6134–6142.

Baalousha, M., Kammer, F., Motelica-Heino, M., Baborowski, M., Hofmeister, C., Lecoustumer, P., 2006. Size-based speciation of natural colloidal particles by flow-field flow fractionation, inductively coupled plasma-mass spectroscopy, and transmission electron microscopy/X-ray energy dispersive spectroscopy: colloids-trace element interaction. Environ Sci Technol 40, 2156–2162.

Baalousha, M., Ju-Nam, Y., Cole, P.A., Gaiser, B., Fernandes, T.F., Hriljac, J.A., Jepson, M.A., Stone, V., Tyler, C.R., Lead, J.R., 2012. Characterization of cerium oxide nanoparticles-part 1: size measurements. Environ. Toxicol. Chem. 31, 983–993.

Baalousha, M., Nur, Y., Römer, I., Tejamaya, M., Lead, J.R., 2013. Effect of monovalent and divalent cations, anions and fulvic acid on aggregation of citrate-coated silver nanoparticles. Sci Tot Environ 454–455, 119–131.

Baalousha, M., Cornelis, G., Kuhlbusch, T.A.J., Lynch, I., Nickel, C., Peijnenburg, W., van den Brink, N.W., 2016. Modeling nanomaterial fate and uptake in the environment: current knowledge and future trends. Environ Sci Nano 3, 323–345.

Domingos, R.F., Baalousha, M., Ju-Nam, Y., Reid, M., Tufenkji, N., Lead, J.R., Leppard, G.G., Wilkinson, K.J., 2009. Characterizing manufactured nanoparticles in the environment-multimethod determination of particle sizes. Environ Sci Technol 43, 7277–7284.

Fabricius, A.L., Duester, L., Meermann, B., Ternes, T.A., 2014. ICP-MS-based characterization of inorganic nanoparticlesΓÇösample preparation and off-line fractionation strategies. Anal. Bioanal. Chem. 406, 467–479.

Frisby, C., Bizimis, M., Mallick, S., 2016. Seawater-derived rare earth element addition to abyssal peridotites during serpentinization. Lithos 248–251, 432–454.

Gondikas, A., von der Kammer, F., Kaegi, R., Borovinskaya, O., Neubauer, E., Navratilova, J., Praetorius, A., Cornelis, G., Hofmann, T., 2018. Where is the nano? Analytical approaches for the detection and quantification of TiO2 engineered nanoparticles in surface waters. Environ Sci Nano 5, 313–326.

Gondikas, A.P., von der Kammer, F., Reed, R.B., Wagner, S., Ranville, J.F., Hofmann, T., 2014. Release of TiO2 nanoparticles from sunscreens into surface waters: a one-year survey at the old Danube recreational lake. Environ Sci Technol 48, 5415–5422.

von der Kammer, F., Ferguson, P.L., Holden, P.A., Masion, A., Rogers, K.R., Klaine, S.J., Koelmans, A.A., Horne, N., Unrine, J.M., 2012. Analysis of engineered nanomaterials in complex matrices (environment and biota): general considerations and conceptual case studies. Environ. Toxicol. Chem. 31, 32–49.

Lead, J.R., Batley, G.E., Alvarez, P.J., Croteau, M.-N., Handy, R.D., McLaughlin, M.J., Judy, J.D., Schirmer, K., 2018. Nanomaterials in the environment: behavior, fate, bioavailability, and effects-An updated review. Environ. Toxicol. Chem. 8, 2029–2063.

Lee, S., Bi, X., Reed, R.B., Ranville, J.F., Herckes, P., Westerhoff, P., 2014. Nanoparticle size detection limits by single particle ICP-MS for 40 elements. Environ Sci Technol 48, 10291–10300.

Li, X., Lenhart, J.J., 2012. Aggregation and dissolution of silver nanoparticles in natural surface water. Environ Sci Technol 46, 5378–5386.

Loosli, F., Berti, D., Yi, Z., Baalousha, M., 2018. Toward a better extraction and stabilization of titanium dioxide engineered nanoparticles in model water. NanoImpact 11, 119–127.

Loosli, F., Wang, J., Rothenberg, S., Bizimis, M., Winkler, C., Borovinskaya, O., Flamigni, L., Baalousha, M., 2019a. Sewage spills are a major source of engineered titanium dioxide release into the environment. Environ Sci Nano 6, 763–777.

Loosli, F., Yi, Z., Wang, J., Baalousha, M., 2019b. Dispersion of natural nanomaterials in surface waters for better characterization of their physicochemical properties by AF4-ICP-MS-TEM. Sci. Total Environ. 682, 663–672.

Mozhayeva, D., Engelhard, C., 2020. A critical review of single particle inductively coupled plasma mass spectrometry – a step towards an ideal method for nanomaterial characterization. J. Anal. At. Spectrom. https://doi.org/10.1039/C9JA00206E.

Navratilova, J., Praetorius, A., Gondikas, A., Fabienke, W., von der Kammer, F., Hofmann, T., 2015. Detection of engineered copper nanoparticles in soil using single particle ICP-MS. Int. J. Environ. Res. Public Health 12, 15756–15768.

Nowack, B., Baalousha, M., Bornhoft, N., Chaudhry, Q., Cornelis, G., Cotteril, J., Gondikas, A., Hasselloev, M., Lead, J.R., Mitrano, D.M., von der Kammer, F., Wontner-Smith, T., 2015. Progress towards the validation of modeled environmental concentrations of engineered nanomaterials by analytical measurements. Environ Sci Nano 2, 421–428.

Oriekhova, O., Stoll, S., 2016. Stability of uncoated and fulvic acids coated manufactured CeO2 nanoparticles in various conditions: from ultrapure to natural Lake Geneva waters. Sci. Total Environ. 562, 327–334.

Pace, H.E., Rogers, N.J., Jarolimek, C., Coleman, V.A., Higgins, C.P., Ranville, J.F., 2011. Determining transport efficiency for the purpose of counting and sizing nanoparticles via single particle inductively coupled plasma mass spectrometry. Anal. Chem. 83, 9361–9369.

Praetorius, A., Gundlach-Graham, A., Goldberg, E., Fabienke, W., Navratilova, J., Gondikas, A., Kaegi, R., Gunther, D., Hofmann, T., von der Kammer, F., 2017. Single-particle multi-element fingerprinting (spMEF) using inductively-coupled plasma time-of-flight mass spectrometry (ICP-TOFMS) to identify engineered nanoparticles against the elevated natural background in soils. Environ Sci Nano 4, 307–314.

Prasad, A., Baalousha, M., Lead, J.R., 2015. An electron microscopy based method for the detection and quantification of nanomaterial number concentration in environmentally relevant media. Sci Tot Environ 537, 479–486.

Ramirez, L., Ramseier Gentile, S., Zimmermann, S., Stoll, S., 2019. Behavior of $TiO_2$ and $CeO_2$ nanoparticles and polystyrene nanoplastics in bottled mineral, drinking and Lake Geneva waters. Impact of water hardness and natural organic matter on nanoparticle surface properties and aggregation. Water 11, 721–734. https://doi.org/10.3390/w11040721.

Rasmussen, K., Mast, J., De Temmerman, P.J., Verleysen, E., Waegeneers, N., Van Steen, F., Pizzolon, J.C., De Temmerman, L., Van Doren, E., Jensen, K.A., 2014. Titanium dioxide, NM-100, NM-101, NM-102, NM-103, NM-104, NM-105: characterisation and physico-chemical properties. JRC science and policy reports 11, 721–734.

Reed, R.B., Martin, D.P., Bednar, A.J., Montano, M.D., Westerhoff, P., Ranville, J.F., 2017. Multi-day diurnal measurements of Ti-containing nanoparticle and organic sunscreen chemical release during recreational use of a natural surface water. Environ Sci Nano 4, 69–77.

Regelink, I.C., Weng, L., Koopmans, G.F., van Riemsdijk, W.H., 2013. Asymmetric flow field-flow fractionation as a new approach to analyse iron-(hydr)oxide nanoparticles in soil extracts. Geoderma 202–203, 134–141.

Römer, I., White, T.A., Baalousha, M., Chipman, K., Viant, M.R., Lead, J.R., 2011. Aggregation and dispersion of silver nanoparticles in exposure media for aquatic toxicity tests. J. Chromatogr. A 1218, 4226–4233.
Singh, C., Friedrichs, S., Ceccone, G., Gibson, N., Jensen, K.A., Levin, M., Goenaga, H., Carlander, D., Rasmussen, K., 2014. Cerium dioxide NM-211, NM-212, NM-213, characterisation and test item preparation. JRC Repository: NM-Series of Representative Manufactured Nanomaterials.
Taurozzi, J.S., Hackley, V.A., Wiesner, M.R., 2012. Preparation of nanoparticle dispersions from powdered material using ultrasonic disruption. NIST Special Publication 1200, 2.
US.EPA, 2002. Methods for Measuring the Acute Toxicity of Effluents and Receiving Water to Freshwater and Marine Organisms. EPA-821-R-02-012, 1–266. U.S. Environmental Protection Agency Office of Water (4303T), Washington, DC (Ref Type: Report).
Venkatesan, A.K., Reed, R.B., Lee, S., Bi, X., Hanigan, D., Yang, Y., Ranville, J.F., Herckes, P., Westerhoff, P., 2018. Detection and sizing of Ti-containing particles in recreational waters using single particle ICP-MS. Bull Environ Cont Toxicol 100, 120–126.
Wang, H., Adeleye, A.S., Huang, Y., Li, F., Keller, A.A., 2015. Heteroaggregation of nanoparticles with biocolloids and geocolloids. Adv. Colloid Interf. Sci. 226 (Part A), 24–36.